Microstructural transitions and growth features in rapid solidification: a comparison between experimental fact and quantitative prediction

H. JONES, Division of Metals, School of Materials, University of Sheffield, Mappin Street, Sheffield S1 3JD, U.K.

Abstract

Microstructural transition has been recognised as a ubiquitous feature of rapid solidification more or less from the outset but progress in the interpretation of such behaviour has been limited until relatively recently. The present contribution reviews this recent progress in understanding based on comparison of quantitative predictions with experimental observations made under conditions of rapid solidification that were well-controlled and well-characterized. It is concluded that, while the extent of agreement between prediction and observation is encouraging so far, further progress will depend on the continued acquisition of definitive experimental information to provide critical tests of theory where no useful measurements presently exist.

Riassunto

La transizione microstrutturale è stata riconosciuta come caratteristica onnipresente della solidificazione rapida sin dall'inizio; tuttavia, fino a poco tempo fa, i progressi nell'interpretazione di tale fenomeno sono stati limitati. Il presente lavoro riesamina il progresso recente nella comprensione basata sul confronto tra le previsioni quantitative e le osservazioni sperimentali effettuate in condizioni di solidificazione rapida attentamente controllate e caratterizzate. Gli Autori concludono sostenendo che, benché la misura dell'accordo tra previsione e osservazione sia incoraggiante, il progresso ulteriore dipenderà dall'acquisizione continua di informazioni sperimentali definitive, allo scopo di fornire test critici della teoria laddove attualmente non esistono misurazioni utili.

1. Introduction

Rapid solidification is now well established as the basis of several types of processing route to achieve

i) constitutional change and/or microstructural refinement with associated improvements in processability and properties,

ii) more economical production of certain product forms such as thin strip or ribbon, filament or fibre, flake or powder, billet preform or a treated surface.

The term rapid solidification can evidently be applied to any process that results in rapid formation of solid (1) and a range of technologies is now available for this purpose including high rate electro-, plasma, sputter-or vapour deposition as well as rapid solidification from the melt. Rapid solidification from the melt has received the most attention to date because it can be quite readily achieved with relatively simple equipment (at least on the laboratory-scale) while being rather widely applicable (especially to metallic materials).

Some constitutional/microstructural effects of rapid solidification that are well-known in metallurgy and materials science include:

a) the grey to white transition in cast irons,

b) chill modification of aluminium-silicon alloys, and

c) glass formation in oxide systems.

In each case the effect requires a critical cooling rate or front velocity to be exceeded during solidification, the magnitude of which is sensitive to material composition. Both (a) and (c) can be modelled essentially in terms of the kinetics of nucleation and growth from the melt of the crystalline phases involved while some key features of (b) remain to be completely defined. One of the early triumphs of rapid solidification was to show that glass formation could occur even in metallic materials (2) provided that the cooling rate was rapid enough to suppress the very effective crystallization processes that normally head off glass formation from metallic melts. Rapid solidification also gives rise to formation of new nonequilibrium crystalline (3) and quasicrystalline phases and to extensions of solid solubility in equilibrium crystalline phases. Quasicrystallinity (4), after metallic glass formation, is the second major discovery to stem from rapid solidification research since its inception as a major activity in the 1960s. Extension of solid solubility by rapid solidification has been known at least since the 1940s (5-7) though progress in modelling and predicting this effect has been limited until quite recently.

Experimental facts concerning such constitutional and associated microstructural effects of rapid solidification generally centre on arrays of *threshold phenomena* e.g. critical levels of cooling rate/sample thickness/droplet size above or below which a specific effect tends to occur. Examples (8, 9) are given in Figures 1 and 2.

Such observations, though of immense practical value, are of only limited use as a basis for testing theoretical predictions which generally require a knowledge of parameters such as growth temperature/undercooling/concentration or front velocity. Examples (10-13) of results presented in this second form are given in Figures 3 and 4, and require experiments to be carried out under conditions in which the internal variable, front velocity, is directly coupled to the external variable, such as withdrawal velocity in Bridgman-type directional solidification (10, 11) or beam traverse velocity in electron beam or laser surface melting (12, 13).

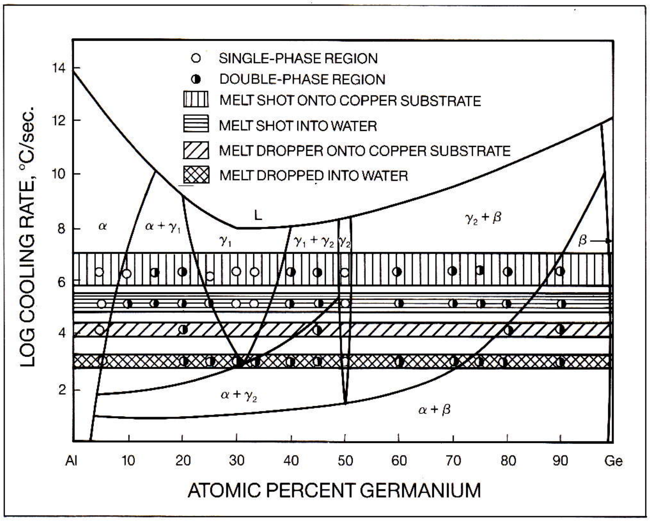

Fig. 1 - Constitution of Al-Ge alloys as a function of estimated cooling rate during solidification. From (8).

Fig. 2 - Fraction amorphous as a function of droplet diameter for two glass-forming Pd-Si alloys. From (9).

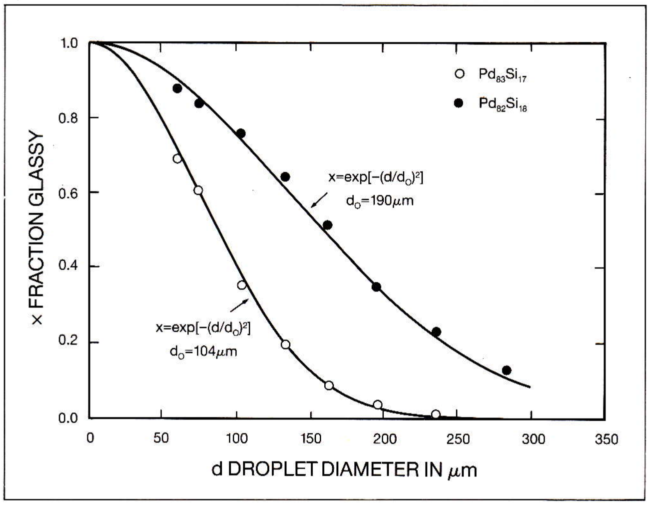

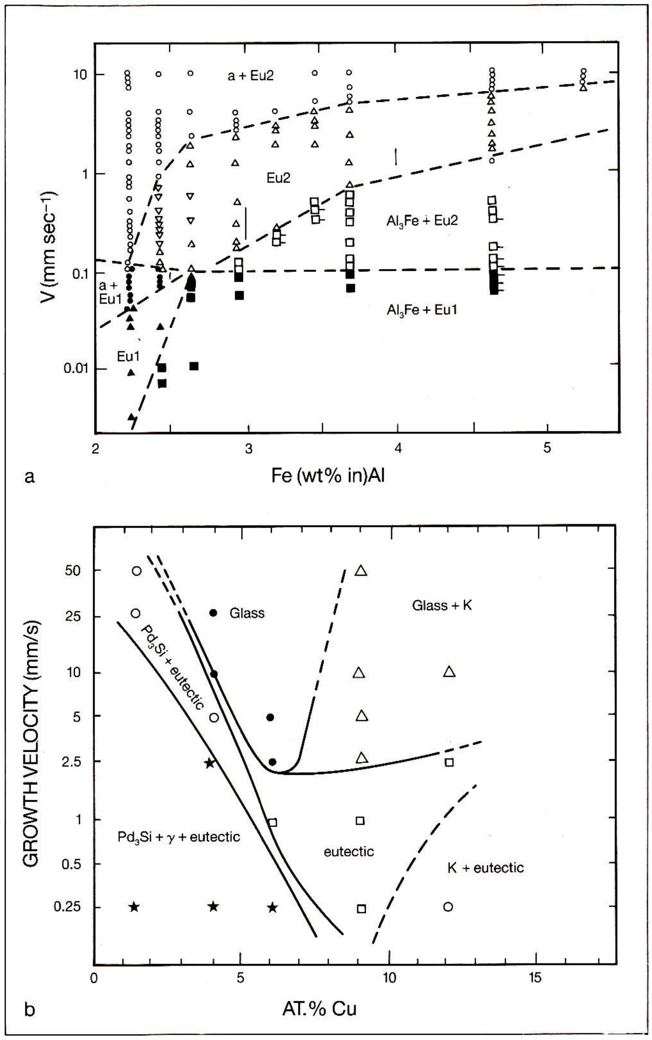

Fig. 3 - Constitution and structure of (a) Al-Fe (10) and (b) Pd-Cu-Si (11) alloys as a function of alloy composition and solidification front velocity V up to 10 or 50 mm/s as determined by Bridgman growth with variable V. Key: Eul = αAl-Al$_3$Fe eutectic; Eu2 = αAl-Al$_6$Fe eutectic.

One goal of the application of theory to rapid solidification is to be able to predict the conditions necessary to generate a particular microstructure in a particular material i.e. the phases (glassy, quasicrystalline or microcrystalline) that will be present, their composition, volume fraction, dimensions and disposition (e.g. primary or eutectic) within the microstructure. The present article is an assessment of how far towards that goal we have progressed over the last decade or so. The article concentrates on modelling of microstructures containing primarily crystalline phases since progress in modelling glass formation has been reviewed repeatedly before e.g. (14-17) while modelling of the requirements for formation of quasicrystalline phases is still at the earliest stage of development (18).

2. Formation of solid solutions

A crucial consideration in the formation of rapidly-solidified microstructures is *composition* of the constituent phases. Conventional phase diagrams display the limiting composition ranges of phases and phase mixtures that are obtainable under *equilibrium* conditions and classical work in *alloy chemistry* by

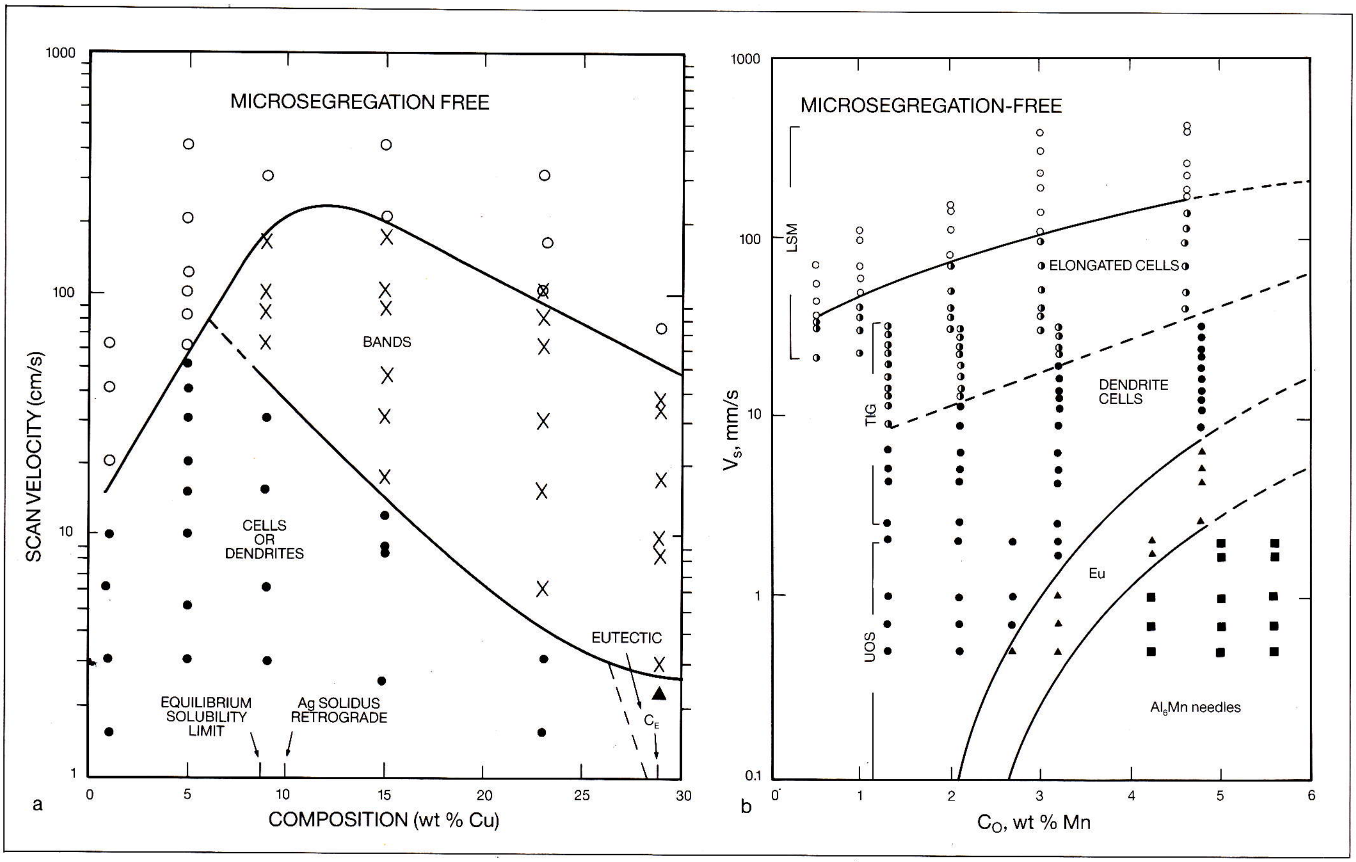

Fig. 4 - Constitution and structure of (a) Ag-Cu (12) and (b) Al-Mn (13) alloys as a function of alloy composition and scan velocity as determined by electron beam (12) or laser (13) surface traverse melting.

Hume-Rothery et al (19) rationalised phase compositions and extents of solid solubility under such conditions in terms of relative atomic sizes and electrochemical characteristics of the constituent atomic species. Hume-Rothery et al concluded that sufficiently large differences in atomic size and electrochemical characteristics resulted in a limited extent of solid solubility and, following the lead of Darken and Gurry (20), two parameter plots of atomic size against, for example, electronegativity or heat of solution, have been employed repeatedly (e.g. [21-27]) to identify ranges of these two parameters within which extensive equilibrium solid solubility in a given solvent is found to occur. Similar plots have been employed also to identify the parametric ranges within which extensive *non*equilibrium solid solubility is found (e.g. [28-31]) and outside which, for example, formation of a glassy phase may replace the crystalline solid solution (e.g. [32-34]). While such plots are of potential value for pinpointing solute elements that, although they show limited equilibrium solid solubility, might exhibit extensive solid solubility under sufficiently extreme conditions of nonequilibrium processing (e.g. rapid solidification), they are not generally capable of predicting the outcome of *particular* experimental conditions of processing.

Firmer limits to the possible outcome of particular conditions can be determined by appropriate application of *thermodynamics*. The importance of the T_0 temperature of a solid phase (at which the free energies of liquid and the solid phase of the same composition are equal) in defining the minimum undercooling required to form the solid phase free of segregation from melt of the same composition is now widely recognised. One implication (35, 36) is that for a system in which T_0 plunges steeply (Figure 5b) it is thermodynamically impossible to form the solid phase free of segregation from melts of concentration exceeding that defined by the plunging T_0. It may still be possible, of course, in this melt concentration range, to form, segregation-free, a *different* solid phase of higher T_0, the other possibility being formation of a glassy phase (37). The extended liquidus and solidus curves of the solid phase under consideration are also important in determining, respectively, the minimum

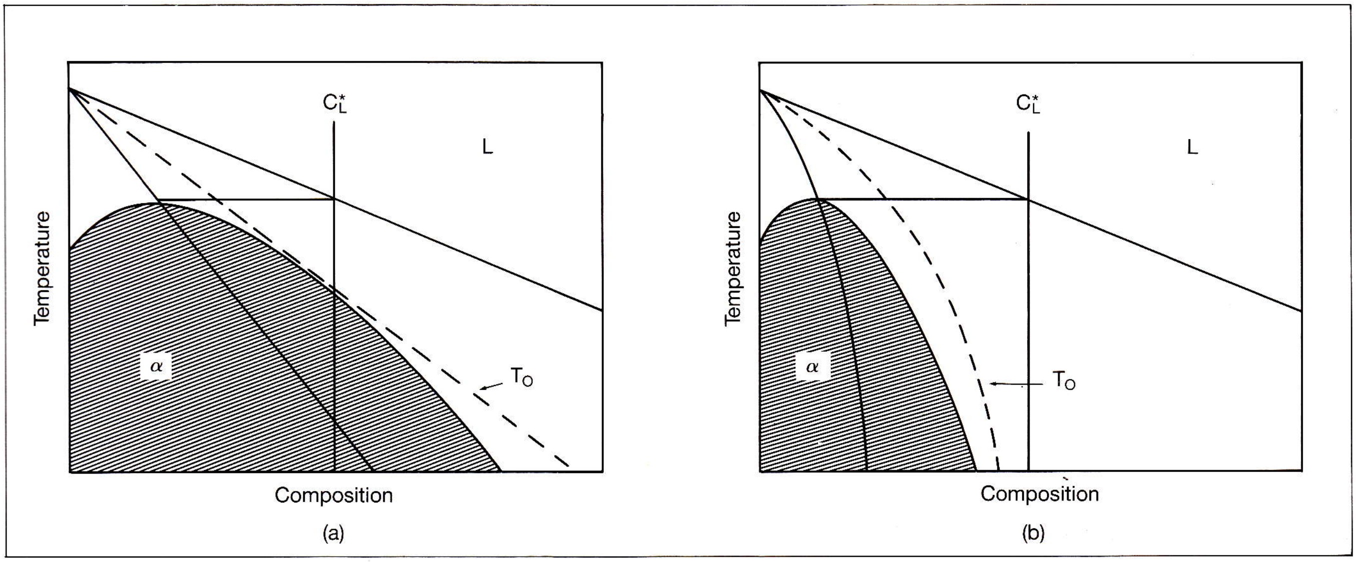

Fig. 5 - Regions (hatched) of thermodynamically permitted compositions of α-phase solidified from liquid of composition C_L^* at various temperature. In (b) segregation-free formation of α is impossible from liquid of composition C_L^* because T_0 for the α-phase does not extend to this concentration. From (35, 36).

undercooling required to form the solid phase from melt of composition such that a different solid phase would form initially under equilibrium conditions, and the melt composition beyond which " solute trapping " (see below) is required for further extension of solid solubility (this arises when the equilibrium or extended solidus displays a retrograde [12, 38, 39]). Once again, prediction of the *actual* outcome of particular conditions is not generally possible by such an approach based on thermodynamic considerations alone.

Further progress along the path towards predicting actual outcomes for specified conditions inevitably must involve *kinetic* considerations. Theoretical treatments of three interrelated phenomena which bear on the formation of solid solutions from alloy melts undergoing rapid solidification have proved to be particularly useful of late for predictive purposes:

i) the stabilization of a " planar " interface at sufficiently high solidification front velocity V (absolute stability)
ii) the tendency of the solute partition coefficient k operative at the solidification front to tend towards unity (i.e. no solute partitioning) at sufficiently high V (solute trapping), and
iii) the growth of cells, dendrites and eutectic under conditions approaching the limits of absolute stability and of eutectic growth.

Accomplishments of the application of theoretical treatments of these phenomena include predictions of:

a) the velocity for formation of segregation-free solid, as a function of alloy concentration C_o
b) tip temperature and solid composition in high velocity cellular or dendritic growth as a function of C_o and V
c) characteristic cell and dendrite spacings as a function of C_o and V, and
d) a limiting condition for eutectic growth at high V.

3. Conditions for formation of segregation-free solid

Segregation-free solidification of an alloy melt can result either when steady state planar growth has been established or when the operative solute partition coefficient k is unity. Planar growth from an alloy melt is stabilized at low velocity by absence of constitutional supercooling given by a condition of the form (40)

$$V < V_c = GD/\Delta T_o \qquad (1)$$

where G is temperature gradient, D is diffusivity of solute in the melt and ΔT_o is alloy freezing range at alloy concentration C_o given by

$$\Delta T_o = mC_o(1-k)/k \qquad (2)$$

where m is the liquidus slope and k the operative solute partition coefficient. Imposition of conditions of growth that satisfy eqn. (1) is well-established to eliminate the lateral microsegregation associated with cellular or dendritic solidification at $V > V_c$. Mullins and Sekerka (41) were the first to predict that planar growth could also be stabilized at high velocity, in this case by capillarity, predicting a condition of the type

$$V > V_a = \Delta T_o D / k\Gamma = mC_o (1 - k) D / k^2 \Gamma \qquad (3)$$

where $\Gamma = \sigma / \Delta S$, the ratio of solid-liquid interfacial free energy σ to entropy of melting ΔS. The validity of this prediction has not been tested until very recently. Table 1 shows two sets of results, for Ag-Cu (12) and for Al-Mn (13). Agreement between predicted V_a and observed velocity V_o for segregation free solidification is within a factor of 3 for Ag-Cu and of 7 for Al-Mn.

Better agreement has been obtained for Ag-Cu by identifying the observed V_o with the predicted maximum velocity V_m of dendritic or cellular growth (42), but the lower value this gives would only tend to increase the difference between observed and predicted critical velocities for Al-Mn. Such comparisons, however, are entirely dependant on the values assumed for k, m and D, so that, for example, a change in the value of k for Mn in Al from 0.7 to 0.4 would effectively eliminate the difference between observed V_o and predicted V_a.

Several models (39, 43-45) of the atomistics of attachment to an advancing freezing front predict a functional relationship between k and V of the general form (36):

$$k = (k_o + a_o V/D)/(1 + a_o V/D) \qquad (4)$$

where k_o is the equilibrium partition coefficient and a_o is the interatomic jump distance from liquid to solid. For typical values of k_o, a_o and D, equation (4) predicts a fairly steep rise in k from k_o to unity over a relatively narrow range of V in the range 1 to 10 m/s.

Experimental confirmation of the precise form of the relationship between k and V is presently restricted to solutes in Si (47-52) and Ge (53) (Figure 6) and progress continues to be made towards improving the fit between such measurements and theoretical models (51, 54, 55).

A notable feature of equation (4) is that D/a_o represents a velocity V_t, at which $k = (k_o + 1)/2$, characteristic of the range of V in which k is moving steeply towards unity. For a sufficiently dilute alloy, V_a from equation (3) will be significantly less than V_t so that segregation-free solidification is then limited by V_a (i.e. by absolute stability) rather than by V_t. Since V_a increases with increased level of alloying, the possibility arises that segregation-free solidification can be limited by V_t (i.e. by solute trapping) at sufficiently high C_o. This transition

TABLE 1 - Predicted velocity V_a for absolute stability compared with observed velocity V_o for segregation-free solidification in Ag-Cu (12) and Al-Mn (13) alloys.

Alloy System	Alloy concentration wt%Cu or Mn	V_o m/s	V_a m/s	V_o/V_a
Ag-Cu*	1	0.15	0.25	0.6
	5	0.6	1.27	0.5
	9	0.6/2.0	2.29	0.3/0.9
Al-Mn+	0.5	0.036	0.0053	6.8
	1.0	0.058	0.0102	5.7
	2.0	0.080	0.0204	3.9
	3.0	0.100	0.0306	3.2
	4.6	0.176	0.0469	3.7

* $k = 0.41$, $m = -6.8$K/wt%, $\Gamma = 1.41 \times 10^{-7}$ mK and $D = 1.5 \times 10^{-9}$ m^2/s
+ $k = 0.70$, $m = -0.75$K/'t%, $\Gamma = 1.08 \times 10^{-7}$ mK and $D = 2.4 \times 10^{-9}$ m^2/s

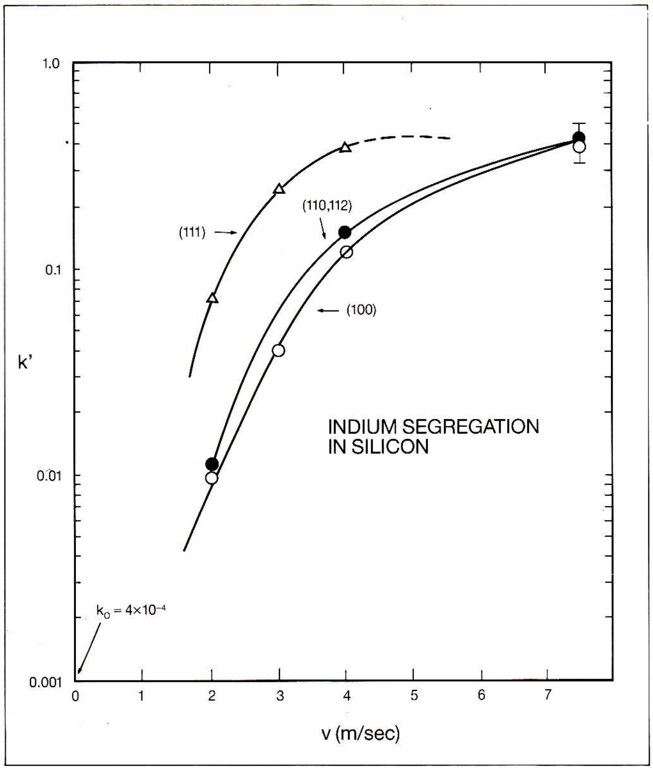

Fig. 6 - Solute partition coefficient k as a function of growth velocity V for indium on different orientations of silicon. From (49).

from limitation by absolute stability to that by solute trapping will occur when $V_a = V_t$ i.e. when (56)

$$C_o = C_o^{CRIT} = k^2\Gamma/m(1 - k)a_o \qquad (5)$$

The data in Table 1 together with $a_o = 0.5$ nm (12) predicts a C_o^{CRIT} of 12wt%Ag for the Ag-Cu system, in excellent accord with the experimental results in Figure 4a, which demonstrate control of segregation-free solidification by absolute stability up to ~ 10wt%Ag and control by solute trapping at concentrations higher than ~ 15wt%Ag. While Figure 4a appears to be the only explicit confirmation of this control transition reported to date, the principle it demonstrates can be usefully applied to other alloy systems. The data in Table 1 for Al-Mn, for example, predicts $C_o^{CRIT} > 100$wt%Mn for Al-Mn indicating that absolute stability controls formation of segregation-free solid at all concentrations in this system. The applicable data for Al-Fe ($k = 0.038$, $m = 3.9$K/wt% and $\Gamma = 1 \times 10^{-7}$ Km [56]), however, predicts a C_o^{CRIT} of 0.08wt%Fe for this system, indicating that solute trapping controls formation of segregation-free solid at all concentrations except for the extremely dilute. This explains convincingly, for the first time, why extension of solid solubility occurs comparatively readily in the Al-Mn system (V_a is no more than ~ 0.1m/s at several percent Mn) while observation of formation of segregation-free solid is so rare (57) for similar percentages of Fe in Al-Fe, requiring the much larger value of V_t (perhaps several m/s or more) to be exceeded. The reason for the relatively low V_a at all concentrations in Al-Mn is notable and stems from its relatively narrow αAl freezing range and lower liquidus slope. The phase diagram parameter $m(1 - k)/k^2$ in equation (5) is thus more than three orders of magnitude larger for Al-Fe than Al-Mn giving rise to V_a some thousands of times larger for Al-Fe than for Al-Mn for the same alloying percentage and to the very low value of C_o^{CRIT} for the Al-Fe system. The tendency to form relatively hard microcellular solid solutions (58) under standard conditions of rapid solidification in systems such as Al-Fe, Al-Co and Al-Ni is a direct consequence. The relatively soft (59) and segregation free solid solutions formed in systems such as Al-Mn, Al-Cr and Al-Zr are correspondingly a result of their relatively small αAl freezing ranges and value of $m(1 - k)/k^2$, which ensures that V_a increases relatively slowly with increasing C_o and so never reaches V_t.

The Ag-Cu, Al-Mn and Al-Fe systems thus illustrate three types of behaviour with respect to formation of segregation-free solid (Figure 7). Type I behaviour (Figure 1a) as exemplified by Al-Mn with low liquidus slope and narrow freezing range, results in $V_a < V_t$ at all C_o so that formation of segregation-free solid is limited by absolute stability at all C_o. Type II behaviour (Figure 1b), as shown by Ag-Cu with moderate αAg freezing range, results in $V_a < V_t$ up to some intermediate C_o beyond which solute trapping limits formation of segregation-free solid. Type III behaviour (Figure 1c) as demonstrated by Al-Fe with very large freezing range, giving a steep rise in V_a on alloying, results in $V_t > V_a$ except for extremely dilute alloys so that solute trapping limits formation of segregation-free solid except at extreme dilution. The very small values of k and associated large ΔT_o characteristic of typical dopants in silicon and germanium will place such systems very firmly into type III so that solute trapping, rather than absolute stability should limit segregation-free solidification at any substantial level of alloying.

4. Conditions at the tip during high velocity cellular or dendritic growth

Standard conditions of rapid solidification tend to result in cellular or dendritic microstructures which are to some degree laterally-segregated rather than segregation-free. A key consideration governing the nature and extent of this (albeit fine-scale) microsegregation is the concentration in the solid at the

Fig. 7 - Illustrating three types of behaviour limiting formation of segregation-free solid as exemplified by schematics of V_a and V_t versus alloy concentration (a) type I, e.g. Al-Mn, in which $V_a<V_t$ at all C_o; (b) type II, e.g. Ag-Cu, for which V_a exceeds V_t beyond some intermediate value of C_o, and (c) type III, e.g. Al-Fe, for which $V_t>V_a$ except for extremely dilute alloying. Absolute stability is limiting in (a) and up to C_o^{CRIT} in (b) and (c) while solute trapping is limiting beyond C_o^{CRIT} in (b) and (c). From (56).

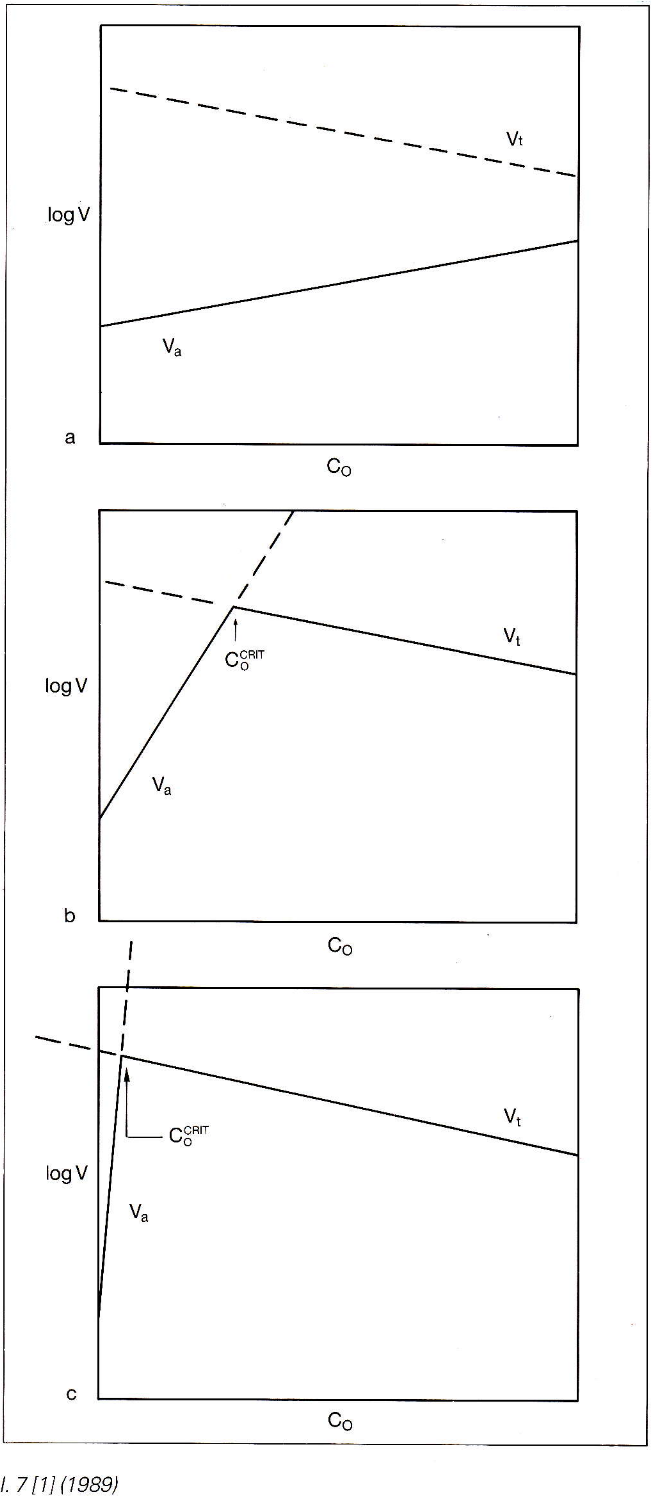

growing cell or dendrite tip, which is, in turn, determined by the temperature of growth of this tip.

Recent developments (42, 60, 61) in the theory of dendritic growth in alloy melts allow the tip temperature T_t, tip concentration C_s^* and tip radius R to be predicted for dendritic and cellular growth as a function of growth velocity and alloy concentration over the range of velocities between V_c and V_a. The fit between measurements (62) and predictions (63) of C_s^* with increase of V up to V_a for the Ag-15wt%Cu alloy is seen to be excellent (Figure 8). Measurements of C_s^* as a function of V are somewhat higher than predictions for Al-1.3 to 3.2wt%Mn alloys (13, 64) though agreement is better for the higher velocities (Figure 9). Measured growth temperatures in the range 0.1 to 2 mm/s are however in excellent agreement with predictions (Figure 10). Some underestimation of C_s^* by the predictions could be anticipated on the basis that the extent of back diffusion of solute into the solid has not yet been taken into account and this is known (65) to have a significant effect on the final C_s of the coarser cellular and dendritic microstructures obtained under normal (nonrapid) solidification conditions. Such considerations of course do not affect measurements of the dendrite or cell tip temperature made in situ during the growth process.

Along with C_s^* or final C_s at the core of the cell or dendrite, the other key consideration concerning microsegregation is the cell or dendrite arm spacing. Cell spacings in rapidly-solidified silicon doped with indium were in reasonable agreement (within a factor of 2) with the fastest growing perturbation wavelength predicted by morphological stability theory (66). In a

Fig. 8 - Tip concentration as a function of growth velocity V for Ag-15wt%Cu according to measurements (62), represented by points, and predictions (63), represented by the continuous line. From (63).

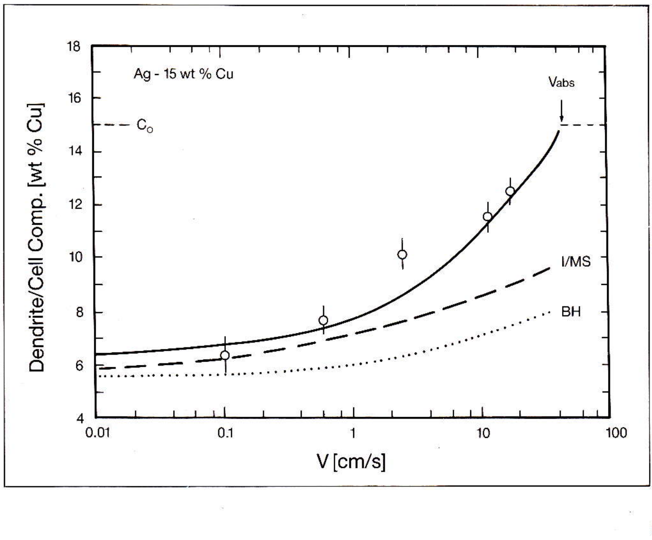

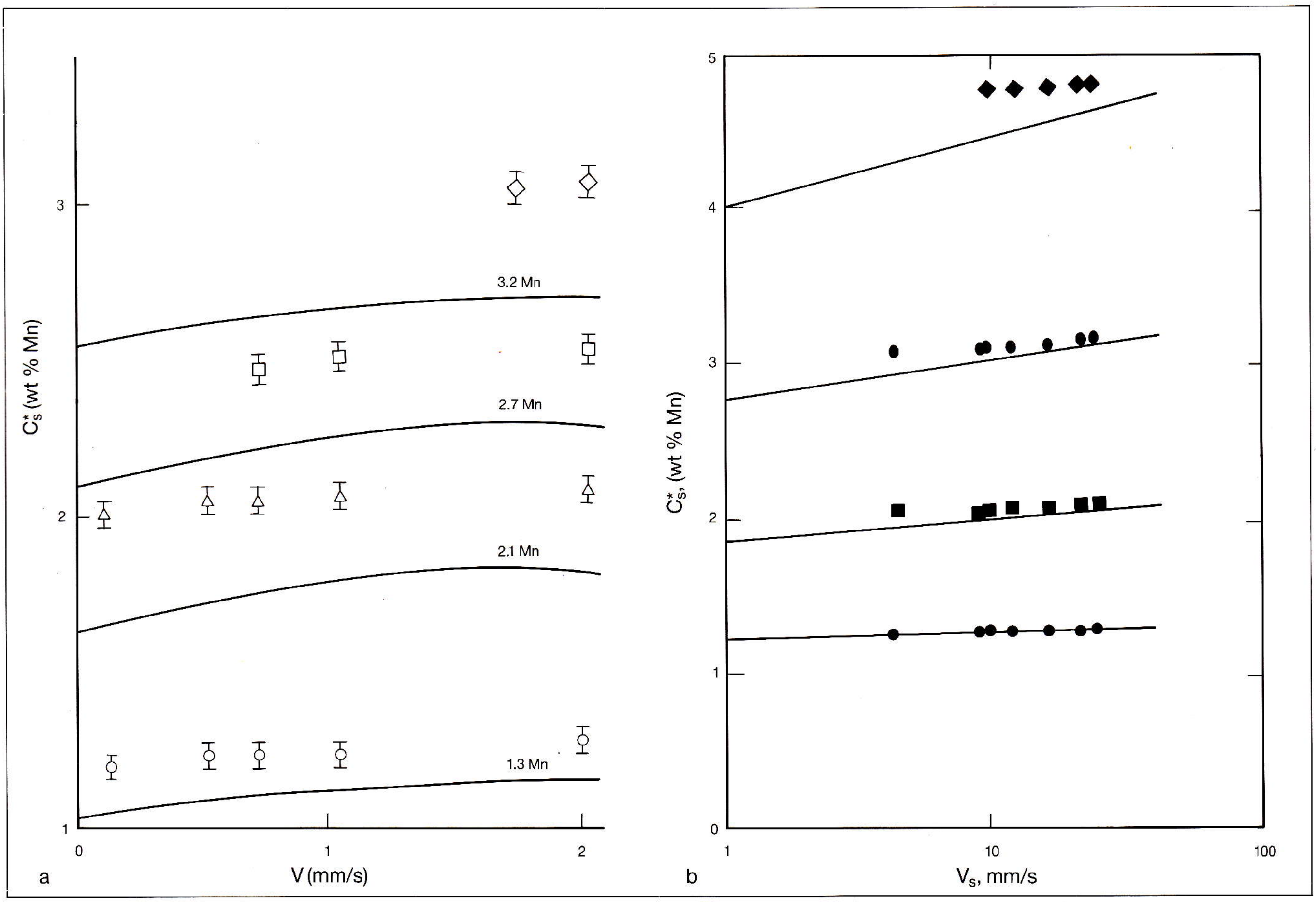

Fig. 9 - Concentration C_s^* of αAl solid solution as a function of growth velocity V and alloy concentration C_o in Al-Mn alloys. (a) Bridgman solidification: ○ 1.3 △ 2.1 □ 2.7 ◇ 3.2 wt%Mn (64). (b) TIG weld traversing: ● 1.3 ■ 2.1 ● 3.2 ◆ 4.8 wt%Mn (13). Points represent measurements while lines are predictions.

different study, agreement between measured cell size and instability wavelength was reported to be closest when the effect of V on k (i.e. solute trapping) was taken into account by the prediction (67). Cell spacings at the limit of absolute stability in Ag-1 and 5wt%Cu were reported to be within a factor of 2 of the predicted wavelength for the onset of instability (12), while cell spacing as a function of growth velocity for Ag-15wt%Cu (Figure 11) was approximately a factor of 3 below this predicted onset wavelength (62). Earlier, good agreement was obtained between measured cell spacings near V_a as a function of V and C_o for Al-Ag alloys and the wavelength for onset of instability (68). Measurements of cell spacing as a function of V and C_o in Al-Mn alloys (13) are generally less than those predicted by the models of Hunt (69) and of Kurz and Fisher (70) with the discrepancy increasing with increase of V (Figure 12). The increase of measured spacing obtained with increasing C_o requires a minimum in the αAl solidus-liquidus curves at some higher value of C_o to be consistent with predictions. Comparison with predicted tip radius R of measured primary spacing λ_1 as a function of V over the range 0.01 to 2 m/s for cellular Al-8wt%Fe alloy obtained by laser surface melt traversing, however, showed encouraging agreement, the measurements of λ_1 being typically of the order of 2R (71). Prediction of dendrite secondary arm spacing as a function of solidification conditions is still a the rudimentary stage. A recent attempt (72) to compare predictions with the power relationship with cooling rate observed for Al-4.5wt%Cu gives reasonable agreement over the range 10^{-3} to 10 K/s but the predicted value (0.25) of the exponent is considerably less than the observed value of 0.37 in this case.

5. Eutectic growth at high velocities

One of the features of chill modification of Al-Si alloys referred to at the outset is that dendrites of αAl appear

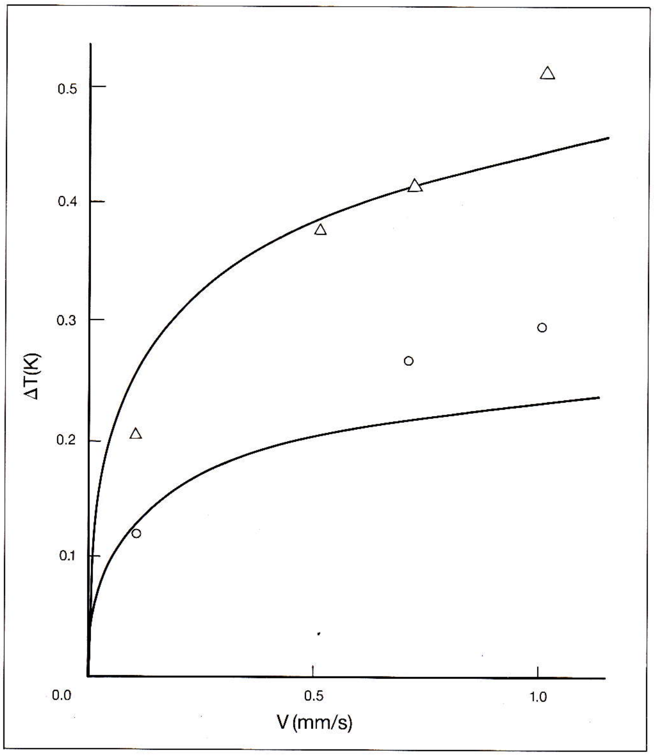

Fig. 10 - Growth undercooling ΔT as a function of velocity V for unextended (○ 1.3wt%Mn) and extended (△ 2.1wt%Mn) αAl solid solutions in Al-Mn alloys. Points represent measurements while lines are predictions (64).

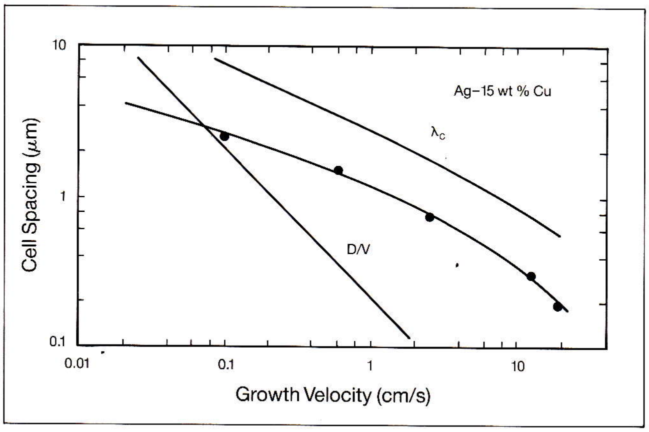

Fig. 11 - Cell spacing as a function of growth velocity for Ag-15wt%Cu alloy compared with wavelength λ_c at the onset of planar instability and "diffusion distance" D/V. From (62).

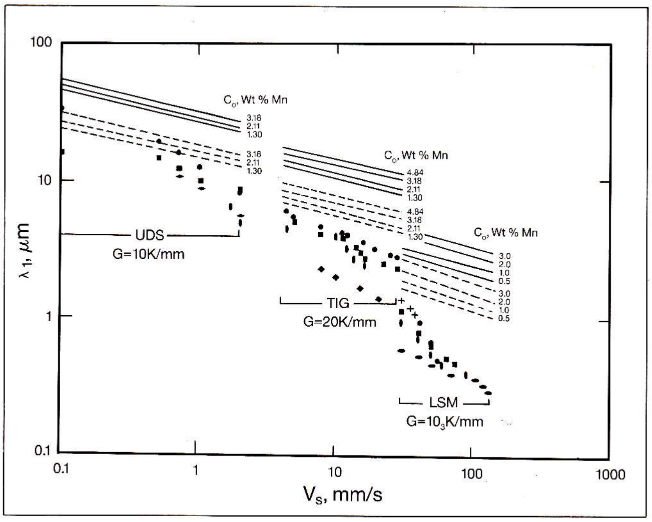

Fig. 12 - Cell spacing λ_1 as a function of growth velocity V and alloy concentration C_0 for Al-Mn alloys for cellular solid solutions obtained by Bridgman (UDS), tungsten inert gas weld (TIG) and laser surface melt (LSM) traversing. Points are measurements and lines are predictions ---- ref. (69) — (70). From (13).

within the eutectic matrix of modified samples of eutectic composition, which are fully eutectic in structure when in the unmodified condition. The implied shift to higher Si-contents of the composition of eutectic growth as a result of chilling is representative of a general phenomenon in eutectic alloy systems. In some cases, as for example in Al-Si, Fe-C, Al-Fe (Figure 3a) and Al-Mn (Figure 4b), fully eutectic growth can proceed within a composition range which shifts to higher concentration with increase of undercooling and growth rate. For other cases such as Al-Cu, Sn-Pb and Fe-Fe_3C, this composition range of fully eutectic growth is broadened (rather than shifted) to embrace compositions on either side of the eutectic composition, corresponding to the broadening which occurs also at low growth rates and undercoolings. The limiting conditions for coupled growth of a eutectic in competition with other phases is that for which the eutectic grows at the same temperature or velocity as one of its constituent phases, another phase or another eutectic. Assuming simple growth laws* for the eutectic and the competing phase, the limiting condition becomes (73):

$$\Delta T_{L/EU} = T_L - T_{EU} = \frac{GD}{V} + BV^n - AV^{1/2} \qquad (6)$$

where n is typically near to 0.5. This equation for a given alloy composition and contending growth forms can have 0, 1 or 2 solutions for V at given G depending on the relative magnitudes of $\Delta T_{L/EU}$, D, B and A. When there are two values V_1, V_2 ($V_1 < V_2$) which satisfy the equation, the smaller one is determined essentially by GD/V and the larger one by $BV^n - AV^{1/2}$. When A is especially large, as is typical for example of

---

Footnote: * For the competing phase $T_L - T = GD/V + BV^n$ where T_L is its liquidus temperature, T is growth temperature and B, n are constants while for the eutectic $T_{EU} - T = AV^{1/2}$ where T_{EU} is eutectic temperature and A is a constant.

morphologically irregular eutectics, such as Al-Si and Fe-C, there may be only one value of V (corresponding to V_1) which satisfies the equation. This results in an absence of fully eutectic growth at high V giving rise to the shift of the composition range for fully eutectic growth to hypereutectic compositions in systems such as Fe-C (74), Al-Si (75), Al-Fe (Figure 3a) and Al-Mn (Figure 4b). This contrasts with Fe-Fe_3C (74), Al-Cu (76), Al-Ni (77), Al-Co (77) and Sn-Pb (78) where A is relatively not so large due to the generally more regular growth modes exhibited by these eutectics.

Experimentally determined limits of coupled eutectic growth as a function of alloy composition, such as Al-Mn (Figure 4b), can be employed in conjunction with other data including measurements of A and/or B to predict the limits of eutectic growth outside the range of measurement (79). Predicted (80) values of A can be used with reasonable confidence when the eutectic is morphologically regular indicating growth at or near the extremum (maximum velocity or minimum undercooling in the predicted relationships between velocity or undercooling with eutectic interlamellar spacing λ). Reliable *measurements* are always to be preferred, however, especially for morphologically irregular eutectics which grow over a range of λ several times that of the extremum value, giving A significantly larger than for the extremum. An interesting feature of the αAl-Al_6Mn eutectic that grows in competition with cellular or dendritic αAl extended solid solution in Al-Mn alloys at high growth velocity is that the eutectic αAl appears to be extended in Mn content to the same level as the competing cellular/dendritic αAl (64). Thus, the fully eutectic structure that grows at 1 mm/s and 3.2wt%Mn contains 3.3 volume percent Al_6Mn in αAl containing 2.1wt%Mn in extended solid solution compared with the 6.2 volume percent that would arise at low velocity with the maximum equilibrium solid solubility of 1.4wt%Mn in the αAl phase.

Measurements of eutectic interlamellar spacing λ and growth undercooling ΔT as a function of growth velocity V for this "extended" Al-3.2wt%Mn eutectic appear to conform to the established parametric relationships $\Delta T/\sqrt{V} = A$ and $\lambda\sqrt{V} = A'$ (Figure 13), for the limited range $0.1 < V < 1$ mm/s investigated and the measured A and A' are within factors of 3 and 2 of their predicted values assuming growth at the extremum. Measurements of λ as a function of V are available, in contrast, over 6 orders of magnitude in V for the Al-Al_2Cu eutectic and show no significant deviation from the single relationship $\lambda\sqrt{V} = 9.4\ \mu m^{3/2}/s^{1/2}$ over the entire range of λ and V (81, 82) (Figure 14). Cline (83) and then Boettinger et al (12, 35) pointed out that the temperature dependence of solute diffusivity D in the supercooled melt would lead to a maximum V for eutectic growth above which the two solid phases could no longer form. More recently, Trivedi et al (84) have argued that values of partition coefficients close to 1 can also give rise to a maximum velocity for eutectic growth by limiting the undercooling that is attainable under the local equilibrium conditions that are expected to be applicable. The limit predicted by this model for the Al-Al_2Cu lamellar eutectic is in excellent agreement with observations (82) from microstructures obtained by laser surface melt traversing (Figure 15). In this instance, banding was observed at velocities above the predicted maximum of 0.5 m/s ($\lambda \sim 6$ nm), a phenomenon observed earlier for the Ag-Cu system (12) which eventually (at 0.5 m/s for Ag-Cu) gave way to formation of microsegregation-free single-phase αAg extended solid solution. A further

Fig. 13 - (a) Growth undercooling ΔT and (b) interphase spacing λ as a function of $V^{1/2}$ for the "extended" αAl-Al_6Mn eutectic containing 3.2wt%Mn. From (64).

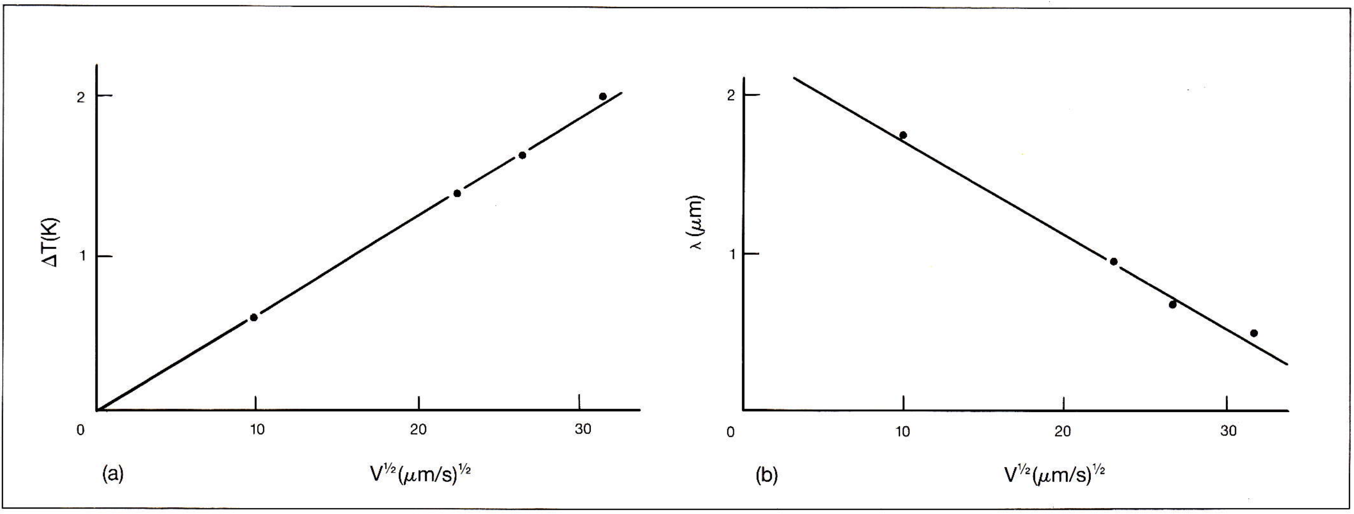

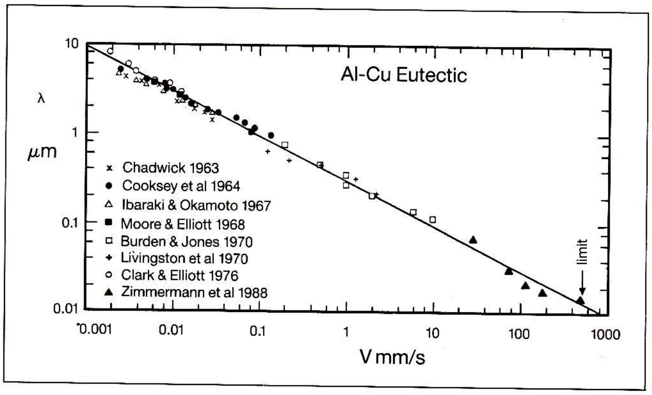

Fig. 14 - Eutectic spacing λ as a function of growth velocity V for Al-Al_2Cu eutectic alloy indicating extinction of stable eutectic separation at V > 500 mm/s. From (81) with results of (82) added.

possibility, shown to occur in the Pd-Cu-Si system (Figure 3b) is that coupled eutectic growth is supplanted by glass formation (11), in this case at the relatively low velocity of 2.5 mm/s.

6. Summing-up

Notable progress has been made of late in successfully applying solidification theory to predict the conditions for microstructural transitions to result from rapid solidification and to account for a number of measurable characteristics of the microstructures resulting from such transitions. These advances have resulted from application of both older and newer theory to mostly newer experimental data obtained under conditions in which local solidification front velocity as high as several m/s was known and well-controlled. Further progress will depend as much as on the judicious extension of the limited amount of definitive experimental data presently available as on further development of applicable theory.

Acknowledgement

The Author is grateful to the following publishers for permission to reproduce previously published material: Chapman and Hall (Figures 1 and 3 [a]), Elsevier (Figures 4 [b], 5, 6, 9 [b] and 12), Metallurgical Transactions (Figure 4 [a]), North-Holland (Figures 7, 8 and 11), Pergamon Press (Figures 2, 9 [a], 10 and 13], The Institute of Metals (Figure 15), The Japan Institute of Metals (Figure 3 [b]) and The Metallurgical Society (Figure 14).

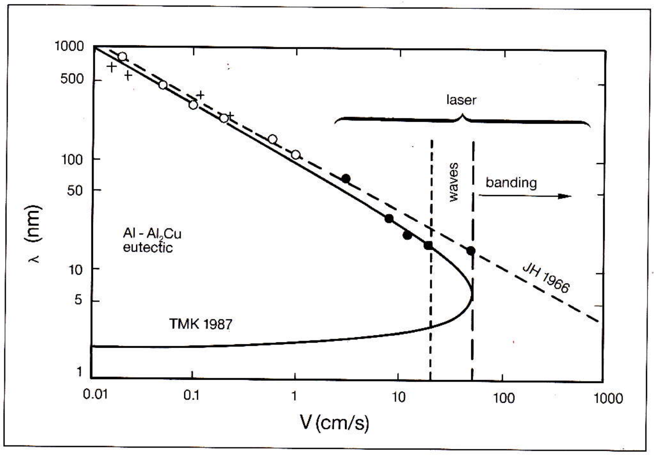

Fig. 15 - Showing predicted maximum in growth rate of lamellar Al-Al_2Cu eutectic in comparison with experimental observations and measurements. From (82). JH1966 = predicted, Jackson and Hunt (80); TMK1987 = Trivedi, Magnin and Kurz (84).

Nomenclature

A	eutectic constant in $T_{EU} - T = AV^{1/2}$
A'	eutectic constant in $\lambda = A'/\sqrt{V}$
B	dendrite constant in $T_L - T = GD/V + BV^n$
a_o	interatomic jump distance from liquid to solid
C_o	alloy composition
C_s^*	tip concentration in solid phase
D	diffusivity of solute in melt
f	fraction segregation-free
G	temperature gradient
k	solute partition coefficient
k_o	equilibrium solute partition coefficient
m	liquidus slope
n	velocity exponent in dendrite eqn. $T_L - T = GD/V + BV^n$
R	tip radius
ΔS	entropy of fusion
T	growth temperature
T_{EU}	eutectic temperature
T_L	liquidus temperature
T_o	melting temperature of partitionless solid
T_t	tip temperature
ΔT	undercooling $T_L - T$ or $T_{EU} - T$
ΔT_o	alloy freezing range $mC_o (1 - k)/k$
$\Delta T_{L/EU}$	temperature interval $T_L - T_{EU}$ (T_L for competing phase)
V	solidification front velocity
V_a	velocity for absolute stability $\Delta T_o D/k\Gamma$
V_c	velocity for conditional stability $GD/\Delta T_o$
V_m	maximum velocity for cellular or dendritic growth
V_o	observed minimum velocity for segregation-free solidification
V_t	velocity D/a_o characteristic of solute trapping
Γ	Gibbs-Thompson parameter $\sigma/\Delta S$
λ	eutectic interphase spacing
λ_1	primary dendrite or cell spacing
σ	solid-liquid interfacial free energy

REFERENCES

*(1) H. Jones, **J. Mater. Sci.**, 1984, **19**, 1043-76.*

*(2) W. Klement, Jr., R.H. Willens and P. Duwez, **Nature**, 1960, **187**, 869-870.*

*(3) P. Duwez, R.H. Willens and W. Klement, Jr., **J. Appl. Phys.**, 1960, **31**, 1137.*

*(4) D. Shechtman, I. Blech, D. Gratias and J.W. Cahn, **Phys. Rev. Lett.**, 1984, **53**, 1951-53.*

*(5) W. Hofmann, **Aluminium**, 1938, **20**, 865-872; W. Hofmann and H. Wiehr, **Z. Metallkunde**, 1941, **33**, 369-372.*

*(6) G. Falkenhagen and W. Hofmann, **Z. Metallkunde**, 1952, **43**, 69-81.*

*(7) P. Duwez, R.H. Willens and W. Klement, Jr., **J. Appl. Phys.**, 1960, **31**, 1136-7 and 1500.*

*(8) C. Suryanarayana and T.R. Anantharaman, **J. Mater. Sci.**, 1970, **5**, 992-1004.*

*(9) A.J. Drehmann and D. Turnbull, **Scripta Met.**, 1981, **15**, 543-8.*

*(10) I.R. Hughes and H. Jones, 1976, **11**, 1781-93.*

(11) W.J. Boettinger, in "Rapidly Quenched Metals", eds. T. Masumoto and K. Suzuki, The Japan Inst. of Metals, Sendai, 1982, pp. 85-88.

*(12) W.J. Boettinger, D. Shechtman, R.J. Schaefer and F.S. Biancaniello, **Met. Trans. A**, 1984, **15A**, 55-66.*

*(13) J. Juarez-Islas, H. Jones and W. Kurz, **Mater. Sci. Eng.**, 1988, **98**, 201-5.*

*(14) H.A. Davies, **Phys. Chem. Glasses**, 1976, **17**, 159-173; **Rev. de Chim. Minerale** 1979, **16**, 349-369; and in "Amorphous Metallic Alloys" ed. F.E. Luborsky, Butterworths, 1983, pp. 8-25.*

(15) F. Sommer, in "Rapidly Quenched Metals", eds. S. Steeb and H. Warlimont, Elsevier, 1985, pp. 153-161.

(16) R.W. Cahn, in "Science and Technology of the Undercooled Melt", eds. P.R. Sahm, H. Jones and C.M. Adam, Martinus Nijhoff, 1986, pp. 73-79.

(17) D.R. Uhlmann, in "Encyclopaedia of Mater. Sci. &. Eng." Vol. 3, Pergamon, 1986, pp. 1980-1983.

*(18) C. Suryanarayana and H. Jones, **Internat. J. Rapid Solidification**, 1988, **3**, 253-293.*

*(19) W. Hume-Rothery, G.W. Mabbott and K.M. Channel-Evans, **Phil. Trans. Roy. Soc. A**, 1934, **A233**, 1-97.*

(20) L. Darken and R. Gurry, in "Physical Chemistry of Metals" McGraw-Hill, New York, 1952, pp. 86-90.

*(21) J.T. Waber, K. Gschneidner, A.C. Larson and M.Y. Prince, **Trans. Met. Soc. AIME**, 1963, **227**, 717-723.*

*(22) V.K. Grigorovich, **Inorg. Mater.**, 1965, **1**, 1556-64.*

*(23) J.R. Chelikowsky, **Phys. Rev. B**, 1979, **B19**, 686-701.*

*(24) J.M. Lopez and J.A. Alonso, **Physica B**, 1982, **113B**, 103-112.*

*(25) J.A. Alonso, J.M. Lopez, S. Simozar and L.A. Girifalco, **Acta Met.**, 1982, **30**, 105-107.*

*(26) H. Jones, **Mater. Sci. Eng.**, 1983, **57**, L5-L8.*

*(27) Z. Bangwei, **Scripta Met.**, 1987, **21**, 1207-11.*

*(28) D.K. Sood and G. Dearnaley, in "Applications of Ion Beams to Materials 1975", eds. G. Carter et al, Inst. Phys. Conf. Ser. No. 28, London, 1976, pp. 196-203; D.K. Sood, **Phys. Lett.**, 1978, **68A**, 469-472.*

*(29) J.A. Lopez and J.A. Alonso, **Phil. Mag. A**, 1982, **45**, 713-722; **Phys. Stat. Sol. (a)**, 1982, **a72**, 777-781.*

(30) V.A. Singh and A. Zunger, **Phys. Rev. B.**, 1982, **B25**, 907-922.

(31) H. Jones, in "Rapidly Solidified Metastable Materials", eds. B.H. Kear and B.C. Giessen, Elsevier, New York, 1984, pp. 303-315.

(32) B.C. Giessen, in "Rapidly Quenched Metals", eds. T. Masumoto and K. Suzuki, The Japan Inst. Met., Sendai, 1982, pp. 213-216.

(33) J.A. Alonso and S. Simozar, **Solid State Commun.**, 1983, **48**, 765-7; S. Simozar and J.A. Alonso, **Phys. Stat. Sol. (a)**, 1984, **a81**, 55-61.

(34) J.A. Alonso, L.J. Gallego and J.M. Lopez, **Phil. Mag. A**, 1988, **58**, 79-92.

(35) W.J. Boettinger, in "Rapidly Solidified Amorphous and Crystalline Alloys", eds. B.H. Kear and B.C. Giessen, Elsevier, New York, 1982, pp. 15-31.

(36) W.J. Boettinger, S.R. Coriell and R.F. Sekerka, **Mater. Sci. Eng.**, 1984, **65**, 27-38.

(37) T.B. Massalski, in "Rapidly Quenched Metals", eds. T. Masumoto and K. Suzuki, The Jap. Inst. Met., 1982, pp. 203-8.

(38) J.C. Baker and J.W. Cahn, **Acta Met.**, 1969, **17**, 575-8.

(39) J.W. Cahn, S.R. Coriell and W.J. Boettinger, in "Laser and Electron beam Processing of Materials", eds. C.W. White and P.S. Peercy, Academic Press, New York, 1980, pp. 89-103.

(40) W.A. Tiller, K.A. Jackson, R.W. Rutter and B. Chalmers, **Acta Met.**, 1953, **1**, 428-437.

(41) W.W. Mullins and R.F. Sekerka, **J. Appl. Phys.**, 1964, **35**, 444-451.

(42) W. Kurz, B. Giovanola and R. Trivedi, **Acta Met.**, 1986, **34**, 823-30.

(43) K.A. Jackson, G.H. Gilmer and H.J. Leamy, as ref. 39, pp. 104-110.

(44) R.F. Wood, **Phys. Rev. B**, 1982, **B25**, 2786-2811.

(45) M.J. Aziz, **J. Appl. Phys.**, 1982, **53**, 1158-68; **Appl. Phys. Lett.**, 1980, **37**, 302-4.

(46) P. Baeri, J.M. Poate, S.U. Campisano, G. Foti, E. Rimini and A. G. Cullis, **Appl. Phys. Lett.**, 1981, **37**, 912-914.

(47) P. Baeri, G. Foti, J.M. Poate, S.U. Campisano and A.G. Cullis, **Appl. Phys. Lett.**, 1981, **38**, 800-802.

(48) C.W. White, in "Laser and Electron Beam Interaction with Solids", eds. B.R. Appleton and G.K. Cellar, N-Holland, Amsterdam, 1982, pp. 109-120.

(49) J.M. Poate, as ref. 48, pp. 121-130.

(50) S.U. Campisano, D.C. Jacobson, J.M. Poate, A.G. Cullis and N.G. Chew, **Appl. Phys. Lett.**, 1985, **46**, 846-8.

(51) M.J. Aziz, J.Y. Tsao, M.O. Thompson, P.S. Peercy and C.W. White, **Phys. Rev. Lett.**, 1986, **56**, 2489-92.

(52) M.J. Aziz and C.W. White, **Phys. Rev. Lett.**, 1986, **57**, 2675-8.

(53) G.J. Clark, A.G. Cullis, D.C. Jacobson, J.M. Poate and M.O. Thompson, in "Laser-Solid Interactions and Transient Thermal Processing of Materials", eds. J. Narayan et al, North-Holland, New York, 1983, pp. 303-310.

(54) L.M. Goldman and M.J. Aziz, **J. Mater. Res.**, 1987, **2**, 524-7.

(55) M.J. Aziz, in "Undercooled Alloy Phases", eds. E.W. Collings and C.C. Koch, The Metallurgical Society Inc., 1987, pp. 375-393; in "Science and Technology of Rapidly Quenched Alloys", eds. M. Tenhover et al, Materials Research Society, Pittsburgh, Pa., 1987, pp. 25-38; **Mater. Sci. Eng.**, 1988, **98**, 369-372.

(56) H. Jones, **Mater. Lett.**, 1988, **6**, 181-2.

(57) M.H. Burden and H. Jones, **Fizika**, 1970, **2** Suppl. 2, Paper 17.

(58) H. Jones, **Mater. Sci. Eng.**, 1969, **5**, 1-18.

(59) A. Fontaine, in "Rapidly Quenched Metals", eds. N.J. Grant and B.C. Giessen, MIT Press, Cambridge, Mass., 1976, pp. 163-167.

(60) J. Lipton, W. Kurz and R. Trivedi, **Acta Met.**, 1987, **35**, 957-64.

(61) R. Trivedi, J. Lipton and W. Kurz, **Acta Met.**, 1987, **35**, 965-70.

(62) W.J. Boettinger, L.A. Bendersky, S.R. Coriell, R.J. Schaefer and F.S. Biancaniello, **J. Cryst. Growth**, 1987, **80**, 17-25.

(63) W. Kurz, B. Giovanola and R. Trivedi, **J. Cryst. Growth**, 1988, **91**, 123-5.

(64) J.A. Juarez-Islas and H. Jones, **Acta Met.**, 1987, **35**, 499-507.

(65) W. Kurz and D.J. Fisher, "Fundamentals of Solidification", **Trans. Tech., Aedermansdorf**, 1986, § 6.5 and Appendix 11.

(66) A.G. Cullis, D.T.J. Hurle, H.C. Webber, N.G. Chew, J.M. Poate, P. Baeri and G. Foti, **Appl. Phys. Lett.**, 1981, **38**, 642-4.

(67) J. Narayan, **J. Appl. Phys.**, 1981, **52**, 1289-93; J. Narayan and C.W. White, in "Rapidly Solidified Amorphous and Crystalline Alloys", eds. B.H. Kear et al, Elsevier, New York, 1982, pp. 553-8.

(68) R.J. Schaefer, W.J. Boettinger, F.S. Biancaniello and S.R. Coriell, in "Lasers in Metallurgy", AIME, 1981, pp. 43-52.

(69) J.D. Hunt, in "Solidification and Casting of Metals", The Metals Society, London, 1979, pp. 3-9.

(70) W. Kurz and D.J. Fisher, **Acta Met.**, 1981, **29**, 11-20.

(71) M. Gremaud, M. Carrard and W. Kurz, to be published.

(72) M.E. Glicksman and N.B. Singh, in "Rapidly Solidified Powder Aluminium Alloys", eds. M.E. Fine and E.A. Starke Jr., ASTM, Philadelphia, Pa., 1986, pp. 44-61.

(73) W. Kurz and D.J. Fisher, **Internat. Met. Rev.**, 1979, **24**, 177-204.

(74) H. Jones and W. Kurz, **Met. Trans. A**, 1980, **11A**, 1265-73.

(75) H.A.H. Steen and A. Hellawell, **Acta Met.**, 1972, **20**, 363-370; D.J. Fisher and W. Kurz, Proc. 6th Internat. Congr. on Light Metals, Aluminium-Verlag, Dusseldorf, 1975, pp. 135-8.

(76) E. Scheil and Y. Masuda, **Aluminium**, 1955, **31**, 51-55.

(77) R.S. Barclay, H.W. Kerr and P. Nielsen, **J. Mater. Sci.**, 1971, **6**, 1168-73.

(78) H.E. Cline and J.D. Livingston, **Trans. Met. Sco. AIME**, 1969, **245**, 1987-92.

(79) J.A. Juarez-Islas and H. Jones, in "Solidification Processing 1987", The Institute of Metals, London, 1988, pp. 492-6.

(80) K.A. Jackson and J.D. Hunt, **Trans. Met. Soc. AIME**, 1966, **236**, 1129-42.

(81) H. Jones, **Mater. Sci. Eng.**, 1984, **65**, 145-156.

(82) M. Zimmermann, M. Carrard and W. Kurz, to be published; quoted by W. Kurz, as ref. 79, pp. 1-12.

(83) H.E. Cline, **J. Appl. Phys.**, 1982, **53**, 4896-4902.

(84) R. Trivedi, P. Magnin and W. Kurz, **Acta Met.**, 1987, **35**, 971-80.